

This is the accepted manuscript made available via CHORUS. The article has been published as:

Reactive Gas Environment Induced Structural Modification of Noble-Transition Metal Alloy Nanoparticles

V. Petkov, L. Yang, J. Yin, R. Loukrakpam, S. Shan, B. Wanjala, J. Luo, K. W. Chapman, and C. J. Zhong

Phys. Rev. Lett. **109**, 125504 — Published 19 September 2012

DOI: [10.1103/PhysRevLett.109.125504](https://doi.org/10.1103/PhysRevLett.109.125504)

Reactive Gas Environment Induced Structural Modification of Noble-Transition Metal Alloy Nanoparticles

V. Petkov^{1,*}, L. Yang², J. Yin², R. Loukrakpam², S. Shan², B. Wanjala², J. Luo², K. W. Chapman³
and C. J. Zhong²

¹Department of Physics, Central Michigan University, Mt. Pleasant, MI 48859, USA

²Department of Chemistry, State University of New York at Binghamton, NY-13902, USA

³X-ray Science Division, Advanced Photon Source, Argonne National Laboratory, Argonne, IL 60439, USA
(August, 2012)

Noble-Transition metal (Noble=Pt, Au; Transition=Co, Ni, Cu) alloy particles with sizes of about 5 nm have been studied by *in situ* high-energy x-ray diffraction while subjected to oxidizing (O₂) and reducing (H₂) gas atmospheres at elevated temperatures. The different gas atmospheres do not affect substantially the random alloy, face-centered-cubic structure type of the particles but affect the way the metal atoms pack together. In O₂ atmosphere atoms get extra separated from each other whereas in H₂ atmosphere they come closer together. The effect is substantial amounting to 0.1 Å difference in the first neighbor atomic distances and concurs with a dramatic change of the particles catalytic properties. It is argued that such reactive gas induced “expansion-shrinking” is a common phenomenon that may be employed for engineering of “smart” nanoparticles responding advantageously to envisaged gas environments.

PACS Numbers: 61.46.Df, 61.05.cf

With current technology moving rapidly toward smaller scales metallic systems have been increasingly produced in nanoscale dimensions and, by employing of various post-synthesis techniques, attempted to be further optimized aiming at enhancing of functional properties. Noble-Transition Metal (Noble=Pt, Au; TM=Co, Ni, Cu) stands out as a particular system of interest because of its great potential for bio-medical [1], optical [2], magnetic [3] and catalytic [4] applications. The unique functionality of nanosized metallic particles arise mostly from quantum size confinement effects that have a profound influence on their atomic-scale structure and, hence, physico-chemical properties. However, nanosized particles (NPs) also have a very large surface to volume ratio and can interact with their environment. Evidence is emerging that when the environment is condensed matter, such as liquid for example, the interaction can be very substantial, including inducing extra strain and modifying the NP’s atomic ordering [5]. Reactive gas environment has been shown to influence the surface chemistry of NPs [6] but little is known about its possible effect on the NPs atomic-scale structure. Successful realization of nanotechnologies depends on good understanding of this effect since NPs are often processed and/or used in reactive gas atmospheres.

In this work we explore a particular application of Noble-TM NPs as catalysts by using *in situ* high-energy x-ray diffraction (XRD) coupled to atomic pair distribution function analysis. The NPs are very stable chemically allowing to concentrate on the effect on the atomic-scale structure alone. We find that these NPs respond very strongly and differently to the different reactive gas atmospheres they are thermally treated in. The packing of the metallic species across the particles loosens when they are thermally treated in O₂-rich

atmosphere. On the other hand, the metal atoms come closer together when treated in reducing, i.e. H₂-rich, atmosphere. Yet no detectable formation of bulk metal-oxide or hydride nanophases is observed in the respective cases. The NPs remain in their “expanded” and “compressed” states when taken out of the respective (O₂/H₂) gas environment and brought back to room temperature indicating that the observed structural modifications are permanent. The “expanded” and “compressed” structure states of Noble-TM NPs concur with profound differences in their catalytic performance indicating a strong reactive gas environment induced - atomic-scale structure state - functional property relationship. This relationship is observed in a range Noble-TM NPs suggesting that it does not depend much on the particular NP’s chemistry and so is likely fairly universal in character. We argue that as such it has to be taken into account in nanocatalysts and other related areas of NPs research.

The synthesis of the binary and ternary alloy NPs studied here followed well established methods involving mixing of appropriate metal precursors in predefined ratios in solution [7]. Thiols/amines and oleic acid/oleylamine compounds were added to the organic solution as capping agents. Once cleaned from the synthesis reaction byproducts, the NPs were mixed with carbon powder in solution. The resulting suspension of carbon supported NPs was dried in N₂. Accounting for the requirements of real-life applications the NPs loading onto carbon was kept close to 10 vol. %. We prepared and studied several binary and ternary Noble-TM alloy NPs. Exploring alloy NPs is essential since Noble metals, in particular Pt, although very useful in catalysis are very scarce and so not very suitable for large-scale applications. Here results for one ternary, Pt₂₅Ni₁₆Co₅₉,

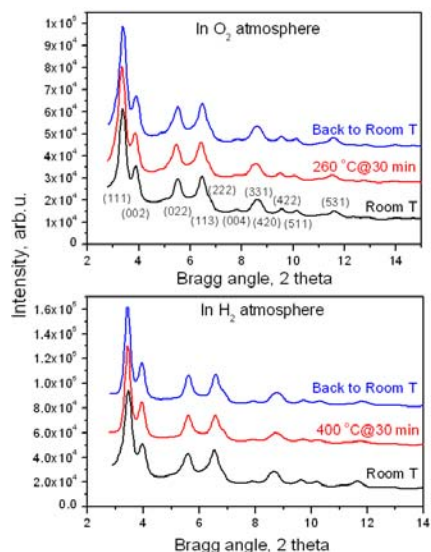


Figure 1. (color online) Experimental XRD patterns for $\text{Pt}_{25}\text{Ni}_{16}\text{Co}_{59}$ NPs taken in O_2 and H_2 atmospheres. Also shown is the temperature at which the data was collected. Diffraction features have been tentatively assigned Miller indexes in a fcc lattice. The assignment, especially at higher Bragg angles, is highly ambiguous because of the features heavy overlap.

and one binary, $\text{Au}_{50}\text{Cu}_{50}$, system are reported only. Note other systems such as $\text{Pt}_{39}\text{Ni}_{22}\text{Co}_{39}$ and $\text{Pt}_{45}\text{V}_{18}\text{Co}_{37}$ were also studied and found to show the reactive gas atmosphere-driven structural modification described here. Results for those systems will be reported elsewhere. The exact NP's compositions were determined by direct current plasma-atomic emission spectroscopy. X-ray photoelectron spectroscopy (XPS) was also used to examine the NPs surface chemical composition. NPs size and morphology was studied by Transition Electron Microscopy (TEM). TEM results showed that the NPs studied here are spherical in shape, and highly monodisperse with an average size of about 5.2(5) nm. Exemplary TEM and XPS data are shown as Supplemental Material in Figs. S1 and S2, respectively.

Typically fresh synthesized NPs are subjected to extra thermal treatment to remove the organic molecules (amines and thiols in our case) capping their surface and only then used in various, in particular catalytic applications. Here we followed two established protocols, namely thermal treatment in oxidizing (80 vol.% N_2 + 20 vol.% O_2) and reducing (95 vol.% N_2 + 5 vol.% H_2) atmospheres. A sample cell described and successfully tested in [8] was used.

In situ high-energy XRD data were collected on the beam line 11-ID-B, at the Advanced Photon Source, Argonne using x-rays of energy 90.48 keV ($\lambda=0.1372$ Å). To improve the XRD data statistics a large area detector was employed. Experimental diffraction patterns for $\text{Pt}_{25}\text{Ni}_{16}\text{Co}_{59}$ NPs are shown in Fig. 1. As can be seen in the Figure the XRD patterns show very broad diffraction features, a picture typical for nanosized materials. The peaks in the XRD patterns shift to higher Bragg angles

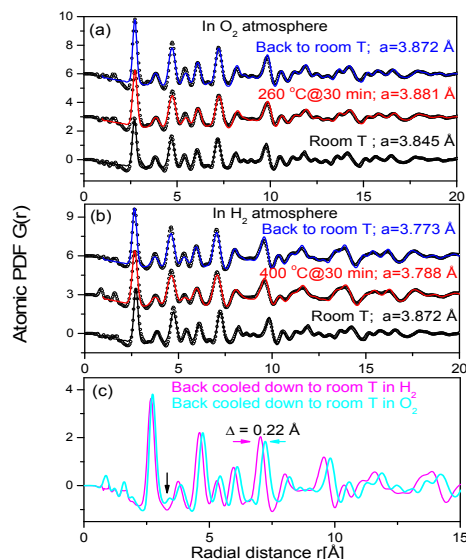


Figure 2. (color online) Experimental (symbols) and model (solid line) atomic PDFs for $\text{Pt}_{25}\text{Ni}_{16}\text{Co}_{59}$ NPs. The refined fcc lattice parameters are given by each data set (a and b). In (c) the experimental PDFs for samples treated in O_2 and H_2 atmosphere are compared to emphasize their different structural states. Vertical arrow marks a feature that may be associated with well expanded Pt-Pt distances due to the formation of metal-oxygen species at the NPs surface [11].

when the sample is treated at 260 °C in O_2 atmosphere for 30 min, and remain shifted at those higher angles even after the sample is cooled down back to room temperature. When the gas atmosphere is changed to reducing (i.e. H_2), the peaks in the XRD patterns hardly shift in position even though this time the sample is heated to considerably higher temperatures (400 °C). The peak shapes do not change substantially in both cases. No new diffraction features appear indicating no formation of new bulk nanophases. The very diffuse character of the Bragg peaks, however, makes it difficult to reveal the exact nature and magnitude of the structural changes taking place in the NPs when exposed to different reactive gas atmospheres. To alleviate the difficulty the XRD data were reduced to their Fourier counterparts, the so-called atomic Pair distribution Functions (PDF)s. High-energy XRD and atomic PDFs have already proven to be very efficient in studying the atomic ordering in NPs [9, 10], including *in situ* studies of NPs during catalytic reactions [8,11].

The experimental PDFs for $\text{Pt}_{25}\text{Ni}_{16}\text{Co}_{59}$ NPs were approached with a structure model featuring an fcc-type atomic ordering that occurs in bulk Noble and Transition metals. As can be seen in Fig. 2 (a, b) the experimental PDF data are almost perfectly fit by this model showing that as obtained and then exposed to different reactive gas environments $\text{Pt}_{25}\text{Ni}_{16}\text{Co}_{59}$ NPs exhibit the same fcc-type atomic structure. No detectable amount of bulk metal oxide or hydride nanophases are revealed by the PDF analysis either. Some very fine features of the PDFs data, in particular a small peak at about 3.3 Å (see the arrow in Fig. 2c) signal the formation of metal-oxide-like

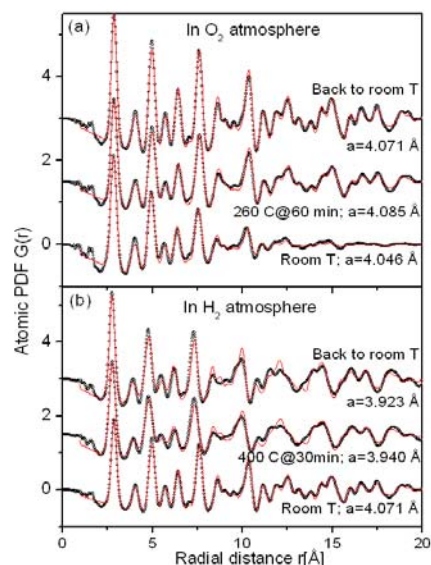


Figure 3. (color online) Experimental (symbols) and model (solid line) atomic PDFs for $\text{Au}_{50}\text{Cu}_{50}$ NPs treated in O_2 (a) and H_2 (b) atmosphere. The refined fcc lattice parameters are given by each data set.

and chemisorbed oxygen species on the very top surface of NPs treated in O_2 atmosphere [11]. No such feature is observed in the PDF data for the sample treated in H_2 atmosphere. What changes much more considerably is the way the metal atoms pack together. The fcc-lattice parameter of $\text{Pt}_{25}\text{Ni}_{16}\text{Co}_{59}$ NPs exposed to O_2 environment changes from $a=3.845$ Å to $a=3.881$ Å at 260 °C and remains expanded at $a=3.872$ Å even when the sample is cooled down back to room temperature, indicating that this expansion is not merely due to the temperature increase but involves a permanent loosening of the atomic packing. When this sample is exposed to H_2 atmosphere, the lattice parameter decreases from the initial value of $a=3.872$ Å (at room T) to 3.788 Å at 400 °C indicating a tightening of the atomic packing. Atoms in $\text{Pt}_{25}\text{Ni}_{16}\text{Co}_{59}$ NPs remain locked in this “compressed” state and, as expected, even come closer together when the sample is cooled down to room temperature ($a=3.773$ Å). Overall the average first neighbor metal-metal distance, as measured from the position of the first PDF peaks (see Fig. 2c) changes from 2.75 Å with the O_2 treated sample to 2.67 Å with the H_2 treated sample. The effect is cumulative and, for example, the sixth neighbor interatomic distances appear at 7.22 Å and 7.01 Å, respectively, amounting to a difference of 0.22 Å (see Fig. 2c). At the same time no substantial change in the NPs bulk and surface (see the XPS data in the Supplemental Materials) chemical composition and NPs shape takes place. Obviously the NPs remain fairly random Noble-Transition metal alloys where atoms are arranged as in a fcc-type structure.

We observed a similar effect with binary $\text{Au}_{50}\text{Cu}_{50}$ NPs. The experimental atomic PDFs obtained in O_2 and H_2 atmospheres are shown in Figs. 3. As obtained $\text{Au}_{50}\text{Cu}_{50}$ NPs have a relatively low degree of crystallinity (see the

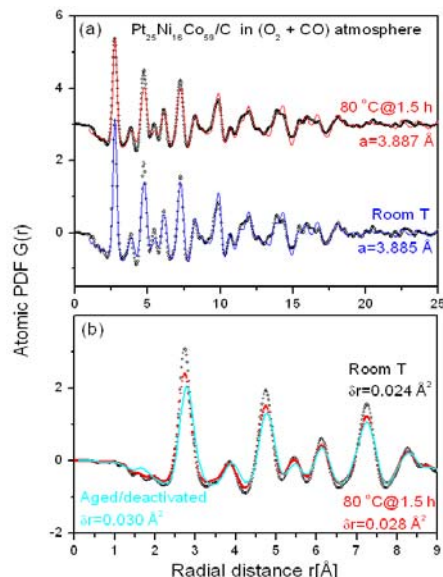


Figure 4. (color online) Experimental (symbols) and model (line) atomic PDFs for $\text{Pt}_{25}\text{Ni}_{16}\text{Co}_{59}$ NPs exposed to a mixture of O_2 and CO at room temperature and at 80 °C for 1.5 h (a). Experimental PDFs of (a) are compared to that of $\text{Pt}_{25}\text{Ni}_{16}\text{Co}_{59}$ that have been subjected to a prolonged aging and so became catalytically inactive. The rms atomic disorder, δr , is seen to increase with the catalyst aging time (b).

fast decay of the PDF peaks above 10 Å in Fig. 3a) yet its atomic ordering can be very well approximated with a model featuring a single nanophase of a fcc-type structure with a lattice parameter $a=4.046$ Å. The NPs remain a single nanophase and become more crystalline in nature when are thermally treated in O_2 atmosphere at 260 °C. The lattice parameter increases to $a=4.085$ Å and the fcc-type ordering remains loosened ($a=4.071$ Å) when the sample is cooled down back to room temperature. When the gas atmosphere is changed to H_2 (see Fig. 3b) a tightening of the atomic packing is observed, and preserved, as indicated by the trend in the refined lattice parameters: from 4.071 Å at room temperature to 3.940 Å at 400 °C and then to 3.923 Å when the sample is cooled down back to room temperature. Here the average first neighbor metal-metal distance, as measured from the position of the first PDF peaks, changes from 2.86 Å with the O_2 treated sample to 2.76 Å with the H_2 treated sample. Obviously, due to their quite different electronegativity, gas species like H_2 and O_2 interact very differently with the NPs surface, including the formation of islands of metal-oxide-like and chemisorbed oxygen species on the very top surface of NPs exposed to O_2 [11,12]. No such species are likely to occur with H_2 . The different interactions propagate into the NPs interior, causing substantial strain (see Supplementary Figures S5-S7) and remarkably opposite in trend overall structural responses. A somewhat similar effect has been observed with semiconductor NPs immersed in liquids of different polarity [5] but our results are the first clear observation with reactive gasses.

The fact that NPs processed in H₂ atmosphere are more compressed, i.e. have, on average, first interatomic distances shorter by ~ 0.1 Å than those in the O₂ atmosphere processed NPs, has a dramatic effect on the catalytic activity for CO oxidation reaction in gas phase and oxygen reduction reaction (ORR) in electrolyte. For example, with the H₂ treated Pt₂₅Ni₁₆Co₅₉ NPs the gas-phase CO conversion rate increases ~ 10 times, and the mass activity for electrocatalytic ORR increases ~ 4 times: from 0.28 to 0.80 A/mg_{Pt} (see Supplemental Materials Figs. S3 and S4, respectively). These results are fully in line with theoretical predictions that shrinking of the metal-metal distances lowers the energy level of the *d*-band electrons with respect to the Fermi level and so decreases the binding energy of CO species to the NPs surface substantially improving the catalytic activity [13]. These results are also consistent with the optimization of the binding energy of O₂ on the alloy catalyst [13] which consequently increases the electrocatalytic activity for ORR. In this respect our study provides very strong and clear experimental evidence in support of these predictions.

The opposite process takes place during CO oxidation reaction. The interaction of the O₂ and CO species with the NPs gradually increases the average metal-metal distances (seen as a shift in the first PDF peak in Fig. 4b) and also introduces extra strain and local structural disorder resulting in asymmetry (see Supplemental Figs. S5-S7) and smearing (see Fig. 4b) of the PDFs peaks. The effect is in line with theoretical predictions [12] and seen even if the NPs catalyst has been used for 1.5 h only (see Fig. 4a) and the catalytic reaction temperature is as low as 80 °C. Eventually, in time, the loosening of the interatomic packing, the extra structural disorder and surface metal-oxide-like species pile up, rendering the NPs inactive as catalysts. Such an inactive catalyst, however, can be fully recovered by a thermal treatment in H₂ atmosphere that not only would clean the NPs surface from CO and O₂ species but, as our study shows, bring the metal atoms closer to interatomic separations that are more favorable for this catalytic reaction.

In summary, reactive gasses, like condensed matter, can interact strongly with Noble-TM particles less than 10 nm in size resulting in a substantial modification of the way the metallic species pack together. When being treated in oxidizing atmosphere the atomic packing of the NPs loosens whereas in reducing atmosphere the atomic packing gets tighter, without changing its random alloy, fcc structure type character. The H₂-gas induced compressed structural state endows Noble-TM NPs with much better catalytic properties. The considerable expansion/shrinking of the first and more distant interatomic distances observed here may also affect the optical and magnetic properties of NPs [14] and so the particular reactive gas environment should definitely be taken into account in NPs research and more thoughtfully

than now made use of. In particular, reactive gas environment induced structural modifications may offer new avenues for engineering of “smart” metallic NPs for catalysis and other applications. One avenue would be to explore for NPs whose structure and, hence, structure-sensitive properties would be modified selectively and advantageously in response to envisaged changes in the gas-phase environment.

This work was supported by DOE Grant DE-SC0006877. Work at APS is supported by DOE under Contract DE-AC02-06CH11357.

Corresponding author: petkov@phy.cmich.edu

- [1] Ch.-An. J. Lin, Ch.-H. Lee, J.-T. Hsieh, H. H. Wang, J. K. Li, J. L. Shen, W. H. Chan, H.-I. Yeh and W. H. Chang, *J. Med. Bio. Eng.*, **29**, 276 (2009).
- [2] P. Mulvaney, *Langmuir* **12**, 788 (1996).
- [3] D. Alloyeau, C. Ricolleau, C. Mottet, T. Oitkawa, C. Langlois, Y. Le Bouar, N. Braidy and A. Loiseau, *Nat. Mat.* **8**, 940 (2009).
- [4] P. Strasser, S. Koh, T. Anniyev, J. Greeley, K. More, Ch. Yu, Z. Liu, S. Kaya, D. Nordlund, H. Ogasawara, M. F. Toney and A. Nilsson, *Nat. Chem.* **2**, 454 (2010).
- [5] H. Zhang, B. Chen, Y. Ren, G. A. Waychunas and J. F. Banfield, *Phys. Rev. B* **81**, 125444 (2010); B. Gilbert, F. Huang, H. Zhang, G. A. Waychunas and J. F. Banfield, *Science* **305**, 651 (2004).
- [6] F. Tao, M. E. Grass, Y. Zhang, D. R. Butcher, J. R. Renzas, Zh. Liu, J. Y. Chung, B. S. Mun, M. Salmeron and G. A. Somorjai, *Science* **322**, 932 (2008).
- [7] M. J. Hostetler, C. J. Zhong, B. K. H. Yen, J. Anderegg, S.M. Gross, N. D. Evans, M. D. Porter, R.W. Murray, *J. Am. Chem. Soc.*, **120**, 9396 (1998); B. Wanjala, R. Loukrakpam, J. Luo, P. N. Njoki, D. Mott, M. Shao, L. Protsailo, T. Kawamura, C. J. Zhong, *J. Phys. Chem., C*, **114**, 17580 (2010); B. Wanjala, B. Fang, R. Loukrakpam, Y. Chen, M. Engelhard, J. Luo, J. Yin, L. Yang, S. Shan, C. J. Zhong, *ACS Catalysis*, **2**, 806 (2012).
- [8] P. J. Chupas, K. W. Chapman, Ch. Kurtz, J. C. Hanson, P. Lee and C. P. Grey *J. Appl. Cryst.* **41**, 822 (2008); S. M. Oxford, P. L. Lee, P. J. Chupas, K. W. Chapman, M.C. Kung and H. Kun, *J. Phys. Chem. C* **114**, 17085 (2010).
- [9] T. Egami and S. J. L. Billinge, *Underneath the Bragg peaks* (Pergamon Press, Amsterdam, 2003).
- [10] V. Petkov, *Mat. Today* **11**, 28 (2008).
- [11] M. A. Newton, K. W. Chapman, D. Thompson and P. J. Chupas, *J. Am. Chem. Soc.* **134**, 5036 (2012).
- [12] D. R. Butcher M.E. Grass, Zh. Zeng, F. Aksoy, H. Bluhm, W.-X. Li, B.S. Mun, G.A. Somorjai and Z. Liu, *J. Am. Chem. Soc.* **133**, 20319 (2011); A.D. Allian, K. Takanabe, K. L. Fajdala, X. Hao, T.J. Truex, J. Cai, C. Buda, M. Neurock and E. Iglesia, *J. Am. Chem. Soc.* **133**, 4498 (2011).
- [13] M. Mavrikakis, B. Hammer, J. K. Nørskov *PRL* **81**, 2819 (1998); M. O. Pedersen, S. Helveg, A. Ruban, I. Stensgaard, E. Laegsgaard, J. K. Nørskov, F. Besenbacher, *Surf. Science* **426**, 395 (1999); J. Greeley, I.E.L. Stephens, A.S. Bondarenko, T. P. Johansson, H. A. Hansen, T. F. Jaramillo, J. Rossmeisl, I. Chorkendorff, J. K. Nørskov, *Nat. Chem.* **1**, 552 (2009).
- [14] A. Sun-Miguel, *Chem. Soc. Rev.* **35**, 876 (2006).
- [15] See Supplemental material at <http://link.aps.org/Supplemental/.....> for TEM and catalytic properties data.

